

**ADSORPTION OF Cr(VI) BY *Zea mays* RACHIS****ADSORCIÓN DE Cr(VI) UTILIZANDO RAQUIS DE *Zea mays***

M.C. Carreño-De León<sup>1</sup>, M. J. Solache.Ríos<sup>2</sup>, I. Cosme-Torres<sup>1</sup>, M.C. Hernández-Berriel<sup>1</sup>, N. Flores-Alamo<sup>1\*</sup>  
<sup>1</sup>Instituto Tecnológico de Toluca, Av. Instituto Tecnológico S/N, Colonia Agrícola Bellavista, C.P. 52149, Metepec, Estado de México, México.

<sup>2</sup>Instituto Nacional de Investigaciones Nucleares, Departamento de Química, Apdo. Postal 18-1027, C.P. 11801 México, D.F., México.

Received June 18, 2015; Accepted December 1, 2016

**Abstract**

Removal of Cr(VI) from aqueous solutions by *Zea mays* rachis (ZMR) was studied. The BET surface area of the *Zea mays* material was  $1.25 \pm 0.01 \text{ m}^2 \text{ g}^{-1}$ , with an average pore size of 4.71 nm. Experimental data show a 100% of Cr(VI) is removed in a period of 4 hours at pH between 1 and 3. A pH value of 3 was chosen for the adsorption studies, with a maximum adsorption capacity of  $2 \text{ mg g}^{-1}$  and a Cr(VI) adsorption percentage onto ZMR of 98.6%. The Freundlich model represented the equilibrium of the adsorption process better than Langmuir model. The adsorption kinetics of Cr(VI) onto ZMR were well defined using the pseudo-second order model. The results showed that ZMR is a potential biomaterial for Cr(VI) removal and pH has an important effect on metal adsorption capacity. The Cr(VI) reduction to Cr(III) was observed during the adsorption process.

**Keywords:** adsorption, Cr(VI), *Zea mays*, adsorption, aqueous solutions.

**Resumen**

En este estudio se investigó la remoción de Cr(VI) en soluciones acuosas con raquis de *Zea mays* (RZM). El área superficial del material resultó de  $1.25 \pm 0.01 \text{ m}^2 \text{ g}^{-1}$ , con un tamaño de poro promedio de 4.71 nm. Los datos experimentales muestran que a valores de pH entre 1 y 3, se remueve el 100% de Cr(VI) en un tiempo de 4 h. Las pruebas de adsorción se realizaron a un pH de 3, obteniéndose una capacidad máxima de adsorción de  $2 \text{ mg g}^{-1}$  y un porcentaje de adsorción de Cr(VI) por RZM de 98.6%. Para los datos de equilibrio se determinó que el proceso de adsorción lo describe mejor la isoterma de Freundlich que la de Langmuir. La cinética de adsorción de Cr(VI) fue descrita adecuadamente por el modelo de pseudo segundo orden. Los resultados obtenidos muestran que el RZM es un biomaterial útil para la adsorción de Cr(VI) y que el pH tuvo un efecto importante sobre la capacidad de adsorción del metal. También se observó que el Cr(VI) tiende a reducirse a Cr(III) en presencia del adsorbente.

**Palabras clave:** adsorción, Cr(VI), *Zea mays*, biosorción, soluciones acuosas.

## 1 Introduction

Chromium exists in the aquatic environment mainly in two states: Cr(III) and Cr(VI). In general, Cr(VI) is more toxic than Cr(III). Cr(VI) affects human physiology, accumulates in the food chain and causes severe health problems ranging from simple skin irritation to lung carcinoma; the International Agency for Research on Cancer (IARC) has classified Cr(VI) as Group 1 (carcinogenic to humans). Hexavalent chromium is of particular environmental concern due to its toxicity and mobility.

It is challenging to remove it from industrial wastewater and is responsible for environmental pollution, toxicity and contamination. The presence of metal ions in natural or industrial wastewater and their potential impact has long been a subject of research in environmental science. Metal ions such as cadmium, chromium, copper, lead, zinc and iron are commonly detected in both natural and industrial effluents and therefore priority is given to regulate these pollutants at discharge level. Adsorption can be a part of the

\* Corresponding author. E-mail: alamofn@gmail.com  
Tel. 01722 2 08 72 00, Ext.: 3432

solution to minimize this problem. Adsorption of heavy metals by bacterial fungal or algal biomass (live or dead cells) and agricultural waste biomass has been recognized as a potential alternative to existing technologies such as precipitation, ion exchange, solvent extraction and liquid membrane for removal of heavy metals from industrial wastewater, since these processes have technical and/or economic constraints (Hasan *et al.* 2007; García-Rosales and Colín-Cruz, 2010; Barrera-Díaz *et al.* 2012). Therefore agricultural waste maize ZMR was chosen for the removal of chromium (VI) from aqueous solutions, because maize bran is easily available, economically viable and biodegradable.

## 2 Materials and methods

### 2.1 Preparation and characterization of adsorbent

The ZMR used as the adsorbent was obtained from Santa Maria Rayon, State of Mexico. The biomaterial was milled and sieved at 60 mesh (0.0098 in), then it was washed several times with double distilled water to remove impurities before drying at 40°C for 72 h. Fourier Transform Infrared Spectroscopy (FTIR) and Brunauer-Emmett-Teller (BET) were used to determine the functional groups and the specific surface area, respectively. Thermogravimetric Analysis (TGA) was used to evaluate the thermal stability. Besides, the material morphology was study by Scanning Electron Microscopy (SEM).

### 2.2 Specific surface area

Specific surface area was determined by the N<sub>2</sub> BET, BELSORP-MAX nitrogen adsorption method at -196°C and a pressure of 76.8 KPa. The dry and degassed samples were then analysed using a multipoint N<sub>2</sub> adsorption-desorption method at 100°C, for 17 h.

#### 2.1.1 Thermogravimetric analysis (TGA)

TGA analysis was used to determine the thermal decomposition of the raw material (organic matter). The area under the DTA curve is proportional to the amount of heat released in the process of exothermic oxidation of organic matter. The sample was placed into a ceramic crucible, and the analysis was carried out under N<sub>2</sub> flow at the heating rate of 10°C min<sup>-1</sup>, with the temperature ranging from room temperature

to 800 °C, by using a TGA instrument Model: LINSEIS1600.

#### 2.1.2 SEM studies

The morphology of the adsorbent was analysed by using with a scanning electron microscope; model JEOL JSM-6610LV at 10 kV. In all cases, the images were obtained with a backscattered electron detector. The elemental chemical compositions of the samples were determined by EDS with an Oxford Pentafet cooled, solid-state device.

#### 2.1.3 Fourier Transform Infrared Spectroscopy (FTIR)

The infrared analysis was performed in the solid samples before and after the adsorption process by using a spectrophotometer Varian Model 640. The samples were scanned from 4000 to 400 cm<sup>-1</sup>. Experiments were also performed alongside the adsorption measurements to investigate the possible complexation between functional groups of the material and chromium ions during the adsorption process.

#### 2.1.4 Effect of pH on adsorption process

Experiments were performed in a batch system by triplicate. 150 mg of adsorbent were left in contact with 15 mL of 20 mg/L of Cr(VI) solutions, pH was previously adjusted to 1, 2, 3, 4, 5 and 6 using NaOH or HCl solutions. The pH was measured with a pH-meter HANNA Instrument HI-221. Continuous stirring for 1h was maintained at 50 rpm 25 °C. Then, the samples were filtered and metal concentrations were measured by using UV-Visible spectrophotometer.

### 2.3 Adsorption study

Adsorption experiments were performed at room temperature (25°C). A 1 M solution of Cr(VI) ions was prepared by dissolving K<sub>2</sub>Cr<sub>2</sub>O<sub>7</sub> (Merck), previously dried in an oven at 105°C for 1 h, in deionized water; the solution was stored in amber glass bottles under refrigeration until use. The adsorption experiments were performed in batch using a solution of 20 mg L<sup>-1</sup> and polypropylene containers. A weight of 150 mg of adsorbent and 15 mL of Cr(VI) solution were used for the experiments. The solid was first hydrated for 3 h at 50 rpm using a Scientific rotary shaker, Model CVP-0228 and then the samples were filtered using Whatman Grade 5 Filter Paper. The solid

phase was dried at room temperature and stored for disposal, while the liquid phase was analyzed using the 1, 5-diphenylcarbazide method to determine the remaining Cr(VI) concentration in sample at 540nm. The samples were analyzed by using a UV-Visible spectrophotometer; model Perkin Elmer Lambda XL5 at a wavelength of 540 nm. Total Cr was measured by Atomic Absorption Spectroscopy and Cr(III) was determined by the difference of total Cr minus Cr(VI), formed during the contact time of Cr(VI) solution and biomass (Dai *et al.* 2012).

## 2.4 Kinetic and equilibrium isotherm models

The pseudo-first order and pseudo-second order models were used for kinetic studies. Freundlich and Langmuir models were used for the equilibrium adsorption studies (Wang and Chen, 2009) between the ZMR adsorbent, Cr(VI) and formed Cr(III) ions.

The pseudo-first order model is represented in Eq. (1):

$$q_t = q_e(1 - e^{-k_1 t}) \quad (1)$$

where  $q_e$  and  $q_t$  are the capacities of adsorption at the equilibrium and at any time  $t$  ( $\text{mg g}^{-1}$ ),  $k_1$  is the rate constant of first order adsorption ( $\text{min}^{-1}$ ). The pseudo-second-order model is represented in Eq. (2):

$$q_t = \frac{k_2 q_e^2 t}{1 + k_2 q_e t} \quad (2)$$

where  $k_2$  is the rate constant of the pseudo-second order equation ( $\text{g mg}^{-1} \text{min}^{-1}$ ).

The Freundlich isotherm supposes a heterogeneous surface with a heat of adsorption non-uniform distributed over the surface. The Langmuir model assumes that adsorption takes place at specific homogeneous sites within the adsorbent, all active sites are energetically equivalent and no interaction occurred between sorbate molecules (Febrianto *et al.* 2009, Cimino *et al.* 2000). The last model is described by the following equation:

$$q_e = \frac{q_{max} b C_e}{1 + b C_e} \quad (3)$$

where  $q_e$  is the removed sorbate concentration at equilibrium ( $\text{mg g}^{-1}$ ),  $C_e$  the sorbate concentration in the aqueous solution at equilibrium ( $\text{mg L}^{-1}$ ),  $q_{max}$  is the maximum adsorption capacity ( $\text{mg g}^{-1}$ ) and  $b$  is the constant related to the affinity of the binding sites ( $\text{L mg}^{-1}$ ).

Eq. (4) represents the empirical Freundlich isotherm based on adsorption on heterogeneous surface:

$$q_e = K_F \cdot C_e^{1/n} \quad (4)$$

where  $K_F$  and  $n$  are the Freundlich constants indicating adsorption capacity ( $\text{mg g}^{-1}$ ) and intensity, respectively.

## 3 Results and discussion

### 3.1 Scanning electron microscopy (SEM) studies and BET surface area

Elemental analysis simultaneously with the morphology of ZMR were determined. The elemental analysis was performed by EDS. The results indicated that the ZMR sample consists mainly of C (47.7%) and O (38.7%), and a lesser percentage of Si (8.1%); an elemental analysis of some white particles found on the sample composed mainly by C and O and to a lesser extent of Si, Al (2.9%), Ca (0.5%), K (0.2%), Fe (0.08%) and Na (1.9%). According to the literature, the presence of these elements is common in biomass due to the mechanism of plant nutrition (Navarro and Lavarro, 2013; Lugo-Lugo *et al.* 2012).

Fig. 1 shows the morphology of biomass after conditioning at magnifications of 1000X and 700X, respectively; they show a similar morphology, a surface with irregular superficial pores of different diameters, 20 to 30  $\mu\text{m}$ , 17 to 19  $\mu\text{m}$  and smaller pores of 2  $\mu\text{m}$ .

The RZM surface had no apparent change after the adsorption process of Cr (Fig. 2), similar porosity and structure were observed; moreover, bright particles from the order of 10 microns were observed which contain chromium. The elemental analysis shown the composition after adsorption: C (51.34%), O (39.03%), Si (4.86%), Cr (0.53%) and Fe (4.24%). The percentages of carbon and oxygen increased, silicon and iron decreased and aluminum disappeared, suggesting a possible ion exchange with aluminum and silicon or possible complexation.

The specific surface area (BET area) of ZMR was  $1.4626 \pm 0.01 \text{ m}^2 \text{ g}^{-1}$  and a mean pore diameter of 4.71 nm, so this material can be classified as mesoporous, these materials have shown some properties that suit for application on adsorption process and environmental remediation due to their excellent periodicities in the mesoporous channels (Showkat, *et al.* 2007, Ramos-Ramirez, *et al.* 2015).

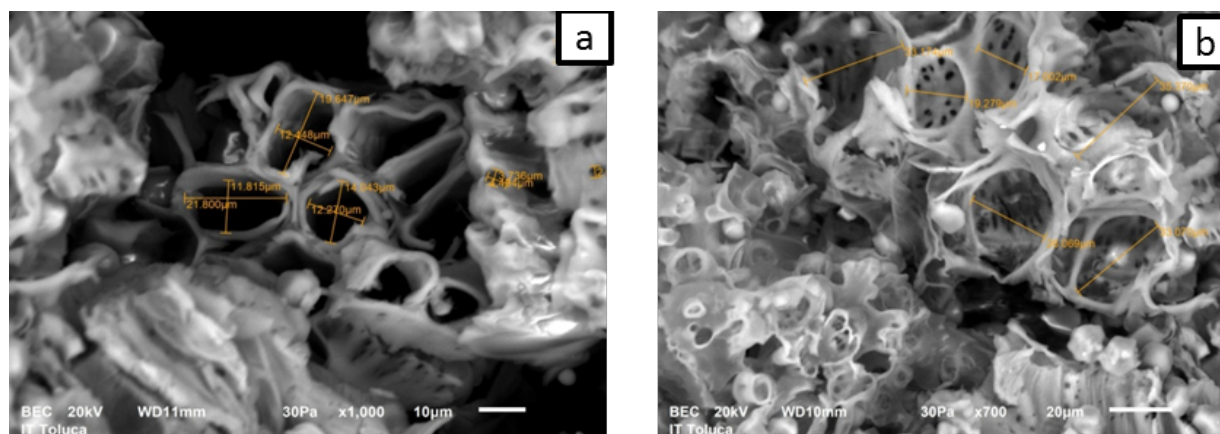


Fig. 1. Micrograph of ZMR conditioning a) 1000X b) 700X.

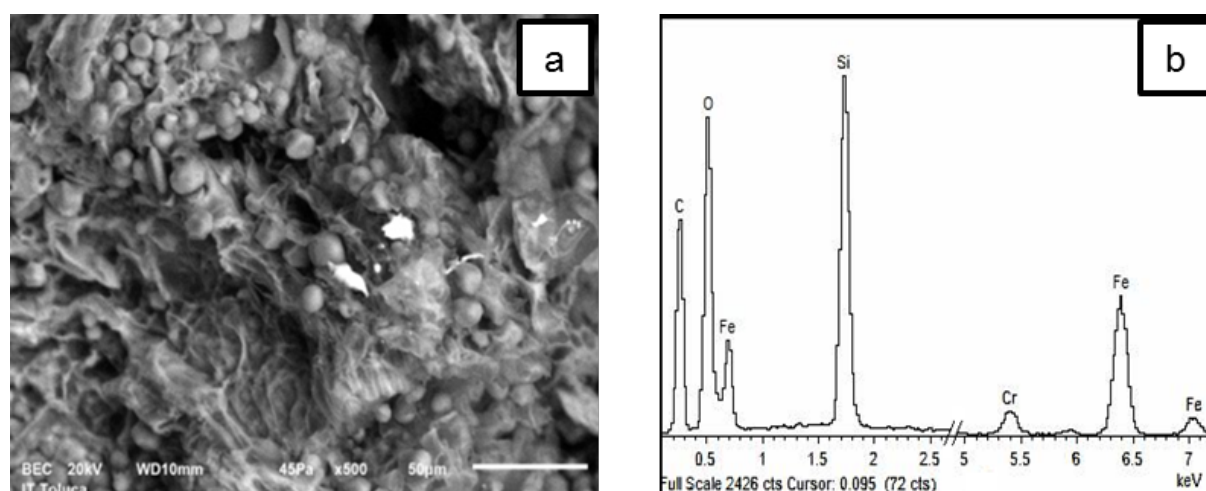


Fig. 2. Thermogravimetric analysis for RZM.

Table 1. Specific area of different adsorbents

Adsorbent	BET Area ( $\text{m}^2 \text{g}^{-1}$ )	Reference
Maize stalk sponge	2.3	García-Rosales and Colín Cruz; (2010)
Sorghum straw	1.2047	García-Reyes and Rangel-Méndez; (2010)
Oat straw	0.9399	García-Reyes and Rangel-Méndez; (2010)
Sawdust	0.86	Gupta and Babu; (2009)
Agave residues	0.5823	García-Reyes and Rangel-Méndez; (2010)
Tea waste	0.39	Malkoc and Nuhoglu; (2007)
Rachis of Zea mays	1.4626	This work

Depending on the value of pore size and according to the IUPAC (Gregg and Sing, 1982; Gunko *et al.* 2013), it can be established that the adsorbent under study is within the classification of mesoporous materials. The BET area was similar to another adsorbents studied (Table 1).

The determination of this feature is very important since porosity allows the diffusion of metal ions

through internal active sites (functional groups) for cations removal (García-Reyes and Rangel-Méndez, 2010).

### 3.2 Thermal stability

The TGA curve (Fig. 3) shows the experimental thermogram of ZMR in the range from 18 to 800°C.

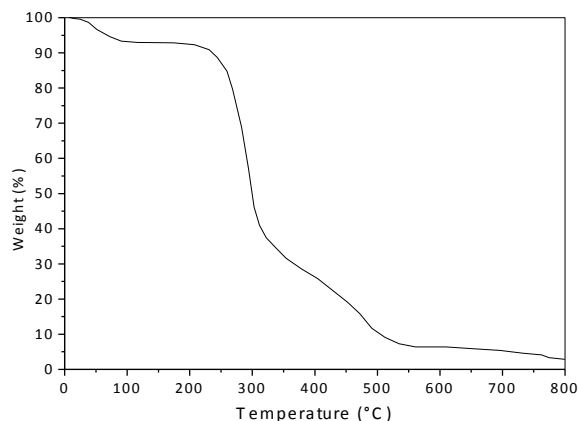


Fig. 3. FTIR spectra of RZM Pristine and RZM-Cr (IV).

The first weight loss step over the temperature range from 21 to 115°C might be due to the loss of residual water in the sample, equivalent to 7% of total weight. In cellulosic materials, endothermic reactions usually result from the generation of non-combustible gases, primarily water vapour, trace amounts of carbon dioxide, formic and acetic acids (Zvinowanda *et al.* 2008).

The second weight loss occurs from 221 to 310°C and was characterized by an important decrease in biomass with a 48% loss. In this stage of the process the volatile low molecular weight compounds are released, which mostly come from hemicellulose (Li X *et al.* 2008). The third stage may be due to the breakdown of high molecular weight compounds such as cellulose and lignin; above 523°C a carbonaceous residue containing fixed carbon and ash is obtained, with a loss of 35% (Tan *et al.* 2010). Thermogravimetric analysis showed that ZMR adsorbent is thermally stable up to around 221°C.

### 3.3 FTIR analysis of ZMR

The FTIR spectrum (Fig. 4) was used to analyze the vibration characteristics of ZMR before and after Cr adsorption. The most representative spectrum bands show the presence of hydroxyl (3400-3200  $\text{cm}^{-1}$ ), esters (1750-1725  $\text{cm}^{-1}$ ), amines (1680-1639  $\text{cm}^{-1}$ ) and alcohols groups (720-590  $\text{cm}^{-1}$ ). The main change observed was a wide band at 3340  $\text{cm}^{-1}$  and this was shifted to 3361  $\text{cm}^{-1}$  that indicates the stretching vibration of OH- groups and their interaction with Cr. Because of the possible complexation between the above functional groups and the metal ions, the stretching vibration of the C-H group at 2922  $\text{cm}^{-1}$  characteristic of cellulose and

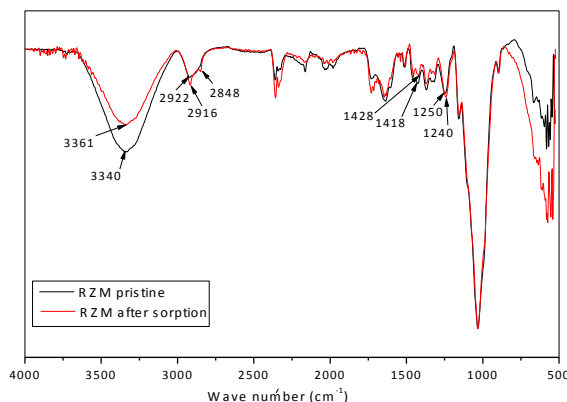


Fig. 4. Adsorption test for Cr(VI) as a function of pH with rachis of ZMR.

lignin was more intense the existence of -CH at 2916  $\text{cm}^{-1}$  and -CH<sub>2</sub> at 2848  $\text{cm}^{-1}$ . The band at 1428  $\text{cm}^{-1}$  was representative of C=C group vibrations and was shifted due to the interaction with OH- groups. At 1250  $\text{cm}^{-1}$  the stretching vibration of the groups (C-O-C), which form part of the cellulose, hemicellulose and lignin suffer a distortion was shifted to 1240  $\text{cm}^{-1}$  (Smith B, 1999; Zvinowanda *et al.*, 2008; Pérez *et al.*, 2010; García-Rosales and Colín-Cruz, 2010; Krishnapriya and Kandaswamy, 2010).

### 3.4 Effect of pH on adsorption process

The pH of solutions is an important parameter on adsorption process because the behaviour of the adsorbent and the chemical species present in solution depend on the pH. The effects of pH on metal uptake capacities are presented in Fig. 5. It is observed that the maximum adsorption capacity ( $q_e$ ) of Cr ions was 2 mg/g at initial pH of 3.

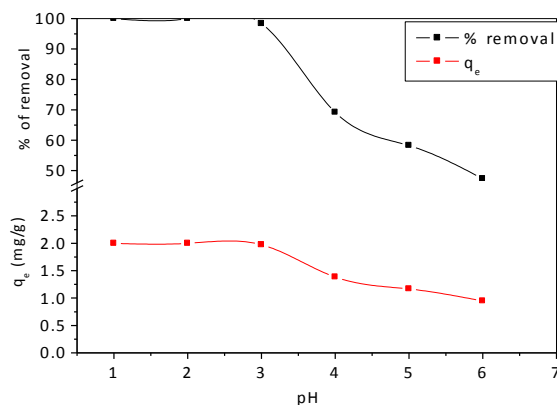


Fig. 5. Adsorption of Cr (VI) in aqueous solution versus contact time with ZMR.

ZMR contains carboxyl, hydroxyl and amine groups that are responsible for Cr removal, adsorption of this metal depends on the protonation or deprotonation of the carboxyl groups. The protonation of the ZMR surface caused by acid medium and the uptake of Cr(VI) is expected to be enhanced at low pH values. The best pH condition for Cr removal was reached at pH of 3, almost 100% of initial Cr(VI) was removed. As the pH value increases over 3, the percentage of Cr(VI) removed decreases up to pH 6 (50 %). This pH value was selected to performed the adsorption experiments because at lower pH values the stability of adsorbent may be affected.

### 3.5 Adsorption of Cr(VI) ions from aqueous solutions

#### 3.5.1 Adsorption kinetic

Fig. 6 shows the adsorption kinetic curves behaviour of Cr(VI) onto ZMR at pH 3 and an initial concentration of 20 mg/L. The maximum adsorption capacity ( $2.00 \text{ mg g}^{-1}$ ) was achieved at equilibrium ( $q_e$ ) in 4 hours of contact time. Experimental data were fitted to pseudo-first and pseudo-second order models to describe the adsorption kinetic behaviour.  $q_{e,exp}$  and the  $q_e$  values are very close to each other for both models, but the calculated correlation coefficients ( $R^2$ ) is higher for pseudo-second order (0.98) than the pseudo-first order kinetic model (0.96) (see Table 2). Therefore, the adsorption data are a little better fitted to pseudo-second order model than the first-order kinetic model for the adsorption of Cr, using ZMR. This last model represents chemical adsorption due to the formation of chemical bonds between adsorbent and sorbate.

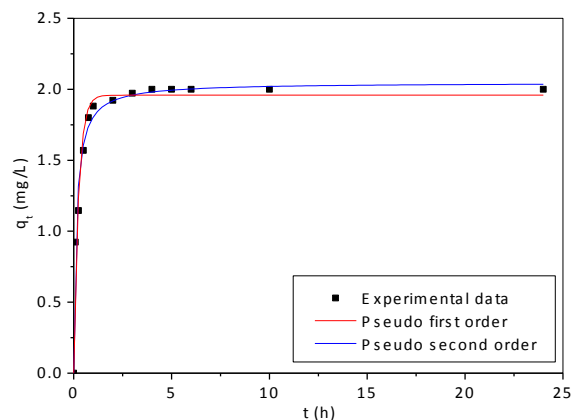


Fig. 6. Adsorption of Cr (VI) in aqueous solution versus contact time with ZMR.

Table 2. Kinetic parameters for Cr (VI) adsorption on Q/PVA/EGDE

Model	T (°C)
	298.15
pseudo first order	
$q_e$ ( $\text{mg}\cdot\text{g}^{-1}$ )	$1.95 \pm 0.04$
$k_1$ ( $\text{h}^{-1}$ )	$4.07 \pm 0.54$
$R^2$	0.96
pseudo-second order	
$q_e$ ( $\text{mg}\cdot\text{g}^{-1}$ )	$2.05 \pm 0.03$
$k_2$ ( $\text{g}\cdot\text{mg}^{-1}\cdot\text{min}^{-1}$ )	$3.64 \pm 0.46$
$R^2$	0.98
$q_{exp}$ ( $\text{mg}\cdot\text{g}^{-1}$ )	2

The pseudo-second order kinetic model has been reported as dominant in adsorption according to studies on the removal of heavy metals in aqueous samples (Flores-Alamo, *et al.*, 2015, García-González, *et al.*, 2016), for example Pandey, *et al.*, (2010) reported a fitting to pseudo-second order kinetic model for Cr(VI) removal using Zeolite NaX. Erhan, *et al.*, (2004) found that the removal of Cr(VI) through agricultural wastes have a pseudo-second order behaviour.

#### 3.5.2 Equilibrium adsorption study

The two predominant oxidation states of chromium are Cr(VI) and Cr(III) and the stability of these species depends on the pH of the system (Cimino *et al.*, 2000). At pH values lower than 3, the dominant specie of Cr is  $\text{HCrO}_4^-$ . Over this pH the  $\text{HCrO}_4^-$  shift to form species like  $\text{CrO}_4^{2-}$  and  $\text{Cr}_2\text{O}_7^{2-}$ , due the presence of a reducing substrates. Cr(VI) is best adsorbed between pH values from 1 to 4.

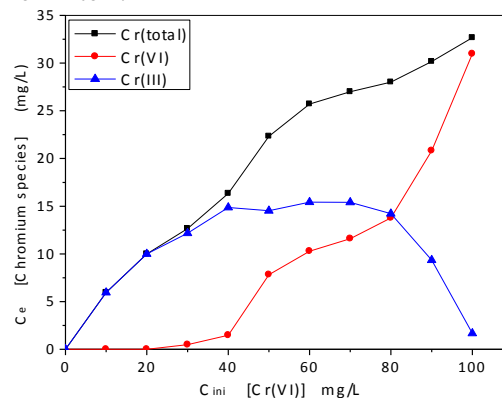


Fig. 7. Concentration profile for chromium species at equilibrium.

Table 3. Isotherm parameters for Cr(VI) adsorption.

Model	Constants	$R^2$
Langmuir	$b$ (L mg <sup>-1</sup> ) $1.16 \pm 0.49$ $q_{max}$ (mg g <sup>-1</sup> ) $6.35 \pm 0.40$	0.93
Freundlich	$K_F$ (mg g <sup>-1</sup> ) $3.27 \pm 0.30$ $n$ $4.50 \pm 0.6$	0.97

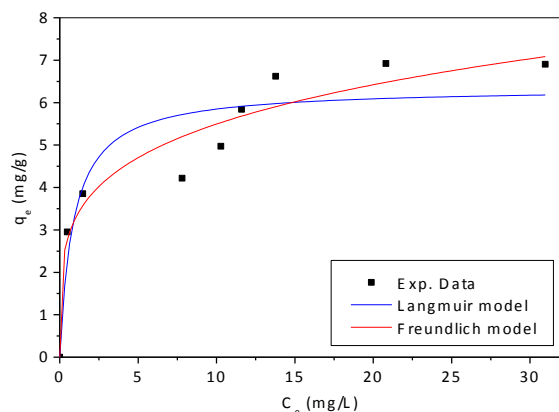


Fig. 8. Langmuir isotherm to adsorption of Cr(VI) on rachis of ZMR.

The equilibrium data, obtained after adsorption process was used to generate a concentration profile for Cr(total), Cr(VI) and Cr(III) (the last one was determined by the difference of the first minus the second).

The trend of the equilibrium concentrations ( $C_e$ ) for Cr (total) and Cr(VI) results similar, since both increase as the initial concentration ( $C_{ini}$ ) of Cr (VI) increases. However, the concentration of Cr(III) increases to a maximum of about 15 mg/L and then a plateau was reached in the range from 40 to 70 mg/L, then it decreases. This behavior suggests that the amount of adsorbent is crucial for the conversion of Cr(VI) to Cr(III), the amount of adsorbent remains constant over all range of  $C_{ini}$ , and adsorbent quantity was not enough to reduce all Cr(VI) at concentrations higher than 20 mg L<sup>-1</sup>.

The experimental data obtained for equilibrium of Cr(VI) adsorption onto ZMR adsorbent were fitted to both models and the equilibrium constants are given in Table 3.

The best fit was found to Freundlich isotherm model with  $R^2$  of 0.97 (Table 3 and Fig. 8), which suggests a multilayer adsorption process and shows the heterogeneity of the adsorbent characteristic of agricultural raw material. The possible mechanism of interaction between Cr(VI) and ZMR adsorbent

might involve both physical and chemical processes as suggested by the results obtained from isotherms and FTIR spectra. Similar results were reported by García-González, *et al.*, (2016).

This adsorption behaviour was similar to the one reported by Dobrowolski and Otto, (2010), who studied Cr(VI) ions adsorption using a modified activated carbon, they found that Freundlich represents the equilibrium behaviour. Pandey *et al.*, (2010) reported a best-fit data to Langmuir model for Cr(VI) removal by using Zeolite NaX.

## Conclusions

The adsorbent material has pores of different sizes, 20-30  $\mu\text{m}$ , 17-19  $\mu\text{m}$  and about 2  $\mu\text{m}$ . The BET specific area of ZMR adsorbent was  $1.46 \pm 0.01$  m<sup>2</sup> g<sup>-1</sup> and a pore diameter about 4.71 nm, a porous material could be benefit to adsorption process. The adsorption process was found to be dependent on initial pH, the adsorption was best accomplished at pH of 3 for Cr(VI) removal. Thermogravimetric analysis showed that ZMR is thermally stable up to 221°C. Kinetic model studies showed that the pseudo-second order model represent the kinetic adsorption behaviour of Cr(VI). The possible mechanism of interaction between Cr(VI) and ZMR adsorbent might involve both physical and chemical processes, and possibly ion exchange with aluminum and silicon, because some bands in the FTIR spectrum shifted after Cr(VI) adsorption experiments. Freundlich isotherm model describes the equilibrium of Cr(VI) removal. A reduction of of Cr(VI) to Cr(III) was observed during the contact with the adsorbent. This biomaterial have good potential as a adsorbent to removal Cr(VI) from aqueous solutions.

## Nomenclature

BET	Brunauer-Emmett-Teller
$b$	constant related to the affinity of the binding sites

$C_{ini}$	$C_e$	sorbate concentration in the initial aqueous solution sorbate concentration in the aqueous solution at equilibrium
EDS		Energy Dispersion Spectroscopy
FTIR		Fourier Transform Infrared Spectroscopy
IUPAC		International Union of Pure and Applied Chemistry
$q_e$		removed sorbate concentration at equilibrium
$q_{max}$		amount of sorbate required to form a monolayer on the adsorbent or concentration to remove
SEM		Scanning Electron Microscopy
TGA		Thermogravimetric Analysis
ZMR		<i>Zea mays</i> rachis

## Acknowledgments

The authors are grateful to Tecnológico Nacional de México for financial support (ITTOL-PTC-006 project).

## References

- Barrera-Díaz C. E, Lugo-Lugo V, Bilyeu. B. (2012). A review of chemical, electrochemical and biological methods for aqueous Cr (VI) reduction. *Journal of Hazardous Materials* 1-12, 224-236.
- Cimino, G., Passerini, A., Toscano, G. (2000). Removal of toxic cations and Cr (VI) from aqueous solution by hazelnut shell. *Water Research* 34, 2955-2962.
- Dai, J., Ren, F., Tao, C. (2012). Adsorption of Cr (VI) and speciation of Cr (VI) and Cr (III) in aqueous solutions using chemically modified chitosan. *International Journal of Environmental Research and Public Health* 9, 1757-1770.
- Demirbas, E., Kobya, M., Senturk, E., Ozkan, T. (2004). Adsorption kinetics for the removal of chromium (VI) from aqueous solutions on the activated carbons prepared from agricultural wastes. *Water S.A.* 30, 533-540.
- Febrianto J., Kosasih A. N., Sunarso J., Yi-Hsu J., Indraswati N., Ismadji S. (2009). Review Equilibrium and Kinetic studies in adsorption of heavy metals using biosorbents. A summary of recent studies. *Journal of Hazardous Materials* 162, 616-645.
- Flores-Alamo, N., Solache-Rios, M. J., Gomez-Espinosa, R. M., and Garcia-Gaitan, B. (2015). Competitive Adsorption Study Of Copper And Zinc In Aqueous Solution Using Q/Pva/Egde. *Revista Mexicana De Ingenieria Química* 14, 801-811.
- García-Reyes R.B., Rangel-Méndez J.R. (2010). Adsorption kinetics of chromium (III) ion san agro-waste materials. *Bioresource Technology* 101, 8099-8108
- García-Rosales G., Colín-Cruz A. (2010). Biosorption of lead by (*Zea mays*) stalk sponge. *Journal of Environmental Management* 91, 2079-2086.
- Gregg S.J. and Sing K. S. (1982). *Adsorption Surface Area and Porosity*. Editorial Academic Press. 2a edición. 111-114.
- García-González, R., Gómez-Espinosa, R. M., Ávila-Pérez, P., Garcia-Gaitán, B., García-Rivas, J. L., y Zavala-Arce, R. E. (2016). Estudio de biosorción de  $Cu^{2+}$  en el criogel quitosano-celulosa. *Revista Mexicana de Ingeniería Química* 15, 311-322.
- Gunko V., Savina I., Mikhlovsky S. (2013). Cryogels: Morphological, structural and adsorption characterization. *Advances in Colloid and Interface Science* 187-188, 1-46.
- Hasan S.H., Singh K. K., Prakash O., Talat M. y Ho Y.S. (2007). Removal de Cr (VI) from aqueous solutions using agricultural waste "maize bran". *Journal Hazardous Materials* 152, 356-365.
- Li X., Tang Y., Cao X., Lu D., Luoland F., Sahao W. (2008). Preparation and evaluation of orange peel cellulose biosorbents for effective removal of cadmium, zinc, cobalt and nickel. *Colloids and Surfaces A. Physicochemical and Engineering Aspects* 317, 512-521.
- Lugo-Lugo V., Barrera-Díaz C., Ureña-Núñez F., Bilyeu B., Linares-Hernández I. (2012). Biosorption of single and binary Cr (III) and Fe (III) system onto pretreated orange peel. *Journal of Environmental Management* 112, 120-127.



- Navarro B. S., Lavarro G.G. (2013). *Química Agrícola: el suelo y los elementos químicos esenciales para la vida*. Ed. Mundi-Prensa Libros S. A. 2ª edición. 15-48.
- Pandey, P. K., Sharma, S. K., Sambhi, S. S. (2010). Kinetics and equilibrium study of chromium adsorption on zeoliteNaX. *International Journal of Environmental Science & Technology* 7, 395-404.
- Ramos-Ramírez, E., Gutiérrez-Ortega, N. L., del Angel-Montes, G., Tzompantzi-Morales, F., Acevedo-Aguilar, F., y Mendoza-Puga, L. E. (2015). Materiales mesoporosos tipo hidrotalcita obtenidos por sol-gel asistido con irradiación de microondas y su evaluación catalítica y adsorbente. *Revista Mexicana de Ingeniería Química* 14, 711-722.
- Showkat, A. M., Zhang, Y. P., Kim, M. S., Gopalan, A. I., Reddy, K. R., Lee, K. (2007). Analysis of heavy metal toxic ions by adsorption onto amino-functionalized ordered mesoporous silica. *Bulletin-Korean Chemical Society* 28, 1985.
- Tan G., Yuan H., Liu Y., Xiao D. (2010). Removal of lead from aqueous solution with native and chemical modified corncobs. *Journal of Hazardous Materials* 174, 740-745.
- Wang, J., Chen, C. (2009). Biosorbents for heavy metals removal and their future. *Biotechnology Advances* 27, 195-226.
- Zvinowanda C.M., Okonkwo J.O., Agyei N.M., Shabalala P.N. (2008). Physicochemical characterization of maize tassel as an adsorbent. I. Surface texture, microstructure and thermal stability. *Journal of Applied Polymer Science* 111, 1923-1930.